

HOW RELIABLE ARE THE AVAILABLE MODELS FOR PREDICTING THE FRP CONTRIBUTION FOR THE SHEAR RESISTANCE OF RC BEAMS?

Gabriel Sas¹ Björn Täljsten², Joaquim Barros³, João Lima³ Fedja Arifovic² and Anders Carolin¹

¹Division of Structural Engineering (SHB)

Luleå University of Technology

971 87 Luleå, Sweden

e-mail: gabriel.sas@ltu.se, anders.carolin@ltu.se

web page: <http://www.ltu.se>

²Division of Structural Engineering (BYG)

Technical University of Denmark

DK-2800 Kgs. Lyngby, Denmark

e-mail: bt@byg.dtu.dk, far@byg.dtu.dk

web page: <http://www.byg.dtu.dk>

³ISISE, School of Engineering, University of Minho

Campus de Azurem, 4800-058 Guimarães, Portugal

e-mail: barros@civil.uminho.pt, joalima@civil.uminho.pt

web page: www.civil.uminho.pt/structures

Keywords: NSMR, EBR, CFRP laminates, CFRP sheets, shear strengthening, reinforced concrete beams, shear models.

Summary: *The performance of the most well-known models for the prediction of the contribution of FRP systems for the EBR shear strengthening of reinforced concrete beams is compared in this paper. The comparison was made using experimental results collected in a large database consisting of approximately 200 FRP strengthened concrete beams with various strengthening configurations and geometric dimensions. The results are not promising and a large scatter between the considered models was obtained. In addition, none of these models predict the ultimate shear capacity very accurately, which is of serious concern considering that some of the models are used in various design codes.*

1 INTRODUCTION

In the last decade intensive research has been conducted on shear strengthening of concrete structures using fiber reinforced polymers (FRP). In the beginning, the majority of the researchers assumed that externally bonded (EBR) FRP materials behave like internal stirrups. Later, studies were focused on developing new theories that take into account the strain field installed in the FRP systems. During the years, many theoretical studies have been carried out. Most of the models use the additional principle that the contribution from the FRP can be added to the ones derived from the stirrups and concrete, not considering any influence of existing strain fields or interaction with steel stirrups. One of the first models to predict the shear contribution of FRP was proposed by Chaallal et al. [1]. The corresponding formulation is based on the assumption that the composite materials and the stirrups have similar behavior. The model assumes that the FRP tensile strength is reached when the composite is intersected by the shear failure crack, if sufficient bond length is available. Malek and Saadatmanesh [2, 3] introduced the anisotropic behavior of the FRP considering the fiber orientation.

Triantafillou [4] and Triantafillou and Antonopoulos [5], based on the computation of an effective FRP strain, and using the truss theory, they derived a model supported from experimental fitting. Khalifa et al. [6, 7] modified Triantafillou's [4] model introducing strain limitations due to shear crack opening and loss of aggregate interlock. The performance of the proposed model was assessed by considering more tests. From the performed tests, Deniaud and Cheng [8, 9] stated that the FRP strains are uniformly distributed among the fibers crossing the crack. A design model was derived combining the strip method and the shear friction approach, based on the failure mechanism observed on the tested specimens. A refined model was proposed in 2004 [10]. Pellegrino and Modena [11] suggested a modified reduction factor for the model of Khalifa et al. [6]. According to the experimental results, the ratio between the steel stirrup and the FRP shear reinforcement percentages has a significant effect on the strengthening effectiveness of FRP systems. Carolin [12] and Carolin and Täljsten [13] presented an equation for predicting the contribution of EBR composites for the shear strengthening. Comparisons between the results recorded from experimental tests and obtained from theoretical models (using measured strains) showed good agreement. The non-uniform distribution of the strains in FRP over the cross section was stated. It must be noticed that anchorage failure was not considered in the present design. Chen and Teng [14, 15, and 16] analyzed the shear failure of reinforced concrete (RC) beams strengthened with FRP and reached the conclusion that the stress (strain) distribution in the FRP along the crack is non-uniform. They presented a model for reinforced concrete beams strengthened with FRP, based on the fiber rupture and debonding. Stress limitation is introduced by bond length coefficient and strip width coefficient. Based on the works of Chen and Teng, new design proposals have been formulated using reduction factors for the ultimate tensile strength and for the spacing between FRP strips. Aprile and Benedetti [17] presented a new flexural – shear design model for RC beams strengthened with EBR FRP systems. This approach combines the modified compression field theory [18] with the variable angle truss model (that takes into account the influence of the FRP systems), in order to predict the contribution of FRP sheets to the shear capacity of RC beams. Although the derivations are coherent, the model has some limitations, since it can only be used for a fully wrapped strengthening scheme, hence the debonding failure mechanism for side bonding strengthening configuration cannot be predicted. Furthermore, the model does not simulate the strain concentration at the composite-crack intersection, so it is unable to foresee the potential rupture of the composite at cracking regions for U wrapping or fully wrapped schemes. Theoretical predictions were compared with experimental results and unfortunately found to be incompatible. Cao et al. [19] proposed an empirical model to predict the FRP contribution to the shear strengthening of RC beams strengthened with FRP wraps failing by FRP debonding. The strain distribution modification factor gave uncertain results, due to the large scatter of the test data. The comparison of the theoretical prediction with the experimental results has shown “a general agreement between the two” with “a significant scatter”. The shear bond model proposed by Zhang and Hsu [20] followed two approaches: model calibration by curve fitting and bond mechanism. The smallest reduction factor for the effective strain obtained from the two methods was suggested to be used. The model for the shear debonding strength developed by Ye et al. [21] has its theoretical starting point in Chen and Teng's model [15], and is now used in the Chinese Design Code. Aspects regarding lateral concrete peeling failure, under shear loading, of FRP were studied by Pellegrino and Modena [22]. This model follows the truss approach and describes the concrete, steel and FRP contribution to the shear capacity of RC beams based on the experimental observations made. Monti and Liotta [23] proposed a debonding model for the FRP-based shear strengthening of RC beams. The features of the model are divided in three steps: generalized constitutive law for the FRP-concrete bond, boundary limitations and shear crack opening provisions. A generalized failure criterion of FRP strips/sheets is introduced. Two cases are considered: straight strip/sheet and strip/sheet wrapped around a corner. The design proposal described in this model is used currently in the Italian design code CNR [24]. The research carried out in the present paper is a step forward from the research performed by Lima and Barros [25].

2 MODELS DESCRIPTION

The present chapter is intended to briefly describe the most well-known models proposed in the last years for the prediction of the EBR FRP contribution for the shear strengthening of RC beams. Due to limitation of space, some models mentioned in the introduction section are not analyzed here.

2.1 Triantafillou

According to Triantafillou [4], and Triantafillou and Antoniadis [5], an accurate estimation of the FRP contribution to the shear capacity is quite difficult to obtain because the failure is dependent on too many factors. The formulation is based on the following equations:

$$V_{frp} = \frac{0.9}{\gamma_{frp}} \rho_{frp} E_{frp} \varepsilon_{frp,e} b_w d (1 + \cot \beta) \sin \beta \quad (1)$$

$$\varepsilon_{frp,e} = 0,0119 - 0,0205 \rho_{frp} E_{frp} + 0,0104 (\rho_{frp} E_{frp})^2, \quad 0 \leq \rho_{frp} E_{frp} \leq 1 \quad (2)$$

$$\varepsilon_{frp,e} = -0,00065 \rho_{frp} E_{frp} + 0,00245, \quad \rho_{frp} E_{frp} > 1 \quad (3)$$

where the meaning of the symbols is presented in the notation list section, at the end of this paper. The model was derived using the truss analogy, based on a semi - quantitative approach. The key parameter of the analytical expression $\varepsilon_{frp,e}$ was obtained from regression of experimental data with beam tests, which may suggest a narrow coverage solution for the shear problem. At this moment no clear distinction was made between the different types of strengthening and the application of the formula. The research was extended on a larger data base of available test reports [5]. The model evolved still based on the regression analysis, but with effective strain for detailed failure types and different strengthening schemes and materials. However, this model cannot simulate the FRP effective strain of the side bonding shear strengthening configuration, which is a serious limitation of its use. Due to the limited data available at the moment of the model's derivation, its prediction accuracy is unsatisfactory.

2.2 Khalifa

Based on the Triantafillou model [4], Khalifa et al. [6, 7] recommended a modified effective strain, both for fiber rupture and debonding failure. The FRP shear contribution to the total capacity of the beam is given by:

$$V_{frp} = \frac{A_{frp} f_{frp,e} (\sin \beta + \cos \beta) d_{frp}}{s_{frp}} \quad (4)$$

By regression of experimental data, the following equation for the ratio of effective stress/strain R was obtained:

$$R = 0.5622 (\rho_{frp} E_{frp})^2 - 1.218 \rho_{frp} E_{frp} + 0.778 \leq 0.5 \quad (5)$$

The R factor was plotted against $\rho_{frp} E_{frp}$ to eliminate the different variation of the thickness of the FRP sheets used in experimental work. Since the derived R may not be valid for debonding failure, Khalifa et al. proposed a bond model approach based on the bond model of Maeda et al. [26]:

$$R = \frac{f_{frp,e}}{f_{frp}} = \frac{0.0042 (f'_c)^{2/3} w_{ef}}{(\rho_{frp} E_{frp})^{0.58} \varepsilon_{frp,u} d_{frp}} \quad (6)$$

The real width parameter, w , was replaced with an effective width w_{ef} to account for several effects such as: shear crack angle (assumed to be 45°), the effective bond and configuration of the strengthening i.e. wrapped, U-jacketing (equation 7a) or side bonded (equation 7b).

$$(a) w_{ef} = d - e^{(6.134 - 0.58 \ln(t_{frp} E_{frp}))} ; (b) w_{ef} = d - 2e^{(6.134 - 0.58 \ln(t_{frp} E_{frp}))} \quad (7a,b)$$

Based on experimental data acquired by Maeda et al. [26] an effective bond length equation was proposed:

$$L_e = e^{6.134 - 0.58 \ln(t_{frp} E_{frp})} \quad (8)$$

Due to its empirical deduction, and the lack of test data at that moment, the effective bond length model is limited. To the final shear capacity of the beam Khalifa et al. suggested a reduction factor of 0.7.

2.3 Chen and Teng

An extensive work performed by Chen and Teng [14, 15, 16] resulted in one of the most used shear models. The general equation is based on the truss model theory, with the remark that discrete FRP strips were modeled as equivalent continuous FRP sheets/plates, and a reduction factor for the stress is used, instead of strain as in the previous models. The general equation of the FRP contribution to the shear capacity is written as:

$$V_{frp} = 2f_{frp,e} t_{frp} w_{frp} \frac{h_{frp,e} (\cot \theta + \cot \beta) \sin \beta}{s_{frp}}, \text{ where } f_{frp,e} = D_{frp} \sigma_{frp,max} \quad (9)$$

The average stress of the FRP intersected by the shear crack, $f_{frp,e}$, is determined based on the assumption that stress distribution in the FRP along the shear crack is not uniform at the ultimate limit state for both rupture and debonding failure modes. The D_{frp} stress distribution factor and the $\sigma_{frp,max}$ maximum stress that can be reached in the FRP intersected by the shear crack are the key factors of the model. The above mentioned parameters are determined for both failure modes as:

$$D_{frp} = \frac{\int_{z_i}^{z_b} \sigma_{frp,z} dz}{h_{frp,e} \sigma_{frp,max}} \text{ or } = \frac{\int_{z_i}^{z_b} \varepsilon_z dz}{h_{frp,e} \varepsilon_{max}} \quad (10)$$

FRP Rupture

Different shapes of non linear distribution of the strains over the crack are considered in the model, similar to the approach found by Carolin [13]. For a general strengthening scheme, the stress distribution factor can be expressed as:

$$D_{frp} = \frac{1 + \zeta}{2} \text{ where } \zeta = z_i / z_b \quad (11)$$

$$z_i = (0.1d + d_i) - 0.1d = d_i, \text{ is the coordinate of the top extremity of the effective FRP} \quad (12)$$

$$z_b = [d - (h - d_c)] - 0.1d, \text{ is the coordinate of the bottom extremity of the effective FRP} \quad (13)$$

When fiber rupture occurs, the maximum stress in the FRP is considered to be the ultimate tensile strength. It was stated that shear failure of the beam may occur before reaching the ultimate tensile failure of the fiber due to the loss of aggregate interlocking.

FRP Debonding

The debonding model developed by Chen and Teng [15] considers as a very important factor the "effective bond length beyond which an extension of the bond length cannot increase the bond strength". The maximum stress in the FRP at debonding is considered to be:

$$\sigma_{frp,max} = \begin{cases} f_{frp} \\ 0.427 \beta_w \beta_L \sqrt{\frac{E_{frp} \sqrt{f_c}}{t_{frp}}} \end{cases}, \beta_L = \begin{cases} 1 & \text{if } \lambda \geq 1 \\ \sin\left(\frac{\pi \lambda}{2}\right) & \text{if } \lambda < 1 \end{cases}, \beta_w = \sqrt{\frac{2 - w_{frp} / (s_{frp} \sin \beta)}{1 + w_{frp} / (s_{frp} \sin \beta)}} \quad (14)$$

Analyzing the model, a dimensional inconsistency of the maximum stress expressed in this mathematical form can be noticed. The reason might be considered to be the fracture mechanic approach and regression analysis on the ultimate bond strength and the FRP width ratio. The two coefficients β_w , β_L , reflect the effective bond length and the effect of FRP to concrete width ratio, respectively. The parameters: normalized maximum bond length λ , the maximum bond length L_{max} and the effective bond length L_e are given as:

$$\lambda = \frac{L_{max}}{L_e}; L_{max} = h_{frp,e} / \sin \beta \text{ for U jacketing, } L_{max} = h_{frp,e} / (2 \sin \beta) \text{ for side bonding and } L_e = \sqrt{\frac{E_{frp} t_{frp}}{\sqrt{f_c}}} \quad (15)$$

In this model it was assumed that all the FRP crossing the shear crack can develop full bond strength. Under this assumption the stress distribution factor for debonding failure was derived (equation 16a). It must be noted as equally important that the bond strength of a strip depends on the distance from the shear crack relative to the ends of the strip. For design purposes a simplified formula was proposed in which 95% characteristic bond strength given by the analytical model is used.

$$(a) D_{frp} = \begin{cases} \frac{2}{\pi \lambda} \frac{1 - \cos \frac{\pi}{2} \lambda}{\sin \frac{\pi}{2} \lambda} & \text{if } \lambda \leq 1 \\ 1 - \frac{\pi - 2}{\pi \lambda} & \text{if } \lambda > 1 \end{cases}; (b) \sigma_{frp,max} = \begin{cases} 0.8 f_{frp} / \gamma_{frp} \\ \frac{0.3}{\gamma_b} \beta_w \beta_L \sqrt{\frac{E_{frp}}{t_{frp}}} \sqrt{f_c} \end{cases} \quad (16a,b)$$

2.4 Zhang and Hsu

The shear bond model proposed by Zhang and Hsu [20] was derived in two steps: model calibration by curve fitting and bond mechanism. The smallest reduction factor, obtained using the two methods, was suggested to be used for the evaluation of the effective strain.

Curve fitting model

To determine the reduction factor for the effective strain when debonding failure occurs, the initial model proposed by Khalifa [6] was used (equation (17a)). With more data collected from test results, a power regression line was used to determine the reduction factor. The power regression gives higher r-square values than the polynomial, which leads to the conclusion that the regression line gives a more realistic equation for the simulation of the structural behavior (equation (17b)).

$$(a) R = \frac{0.0042(f_c')^{2/3} w_{fe}}{(E_{frp} t_{frp})^{0.58} \varepsilon_{fu} d_f}; (b) R = 0.1466(\rho_{frp} E_{frp})^{-0.8193}; (c) R = 1.8589(\rho_{frp} E_{frp} / f_c')^{-0.7488} \quad (17a,b,c)$$

Separate analysis was performed for the debonding and fiber rupture failure modes. A large scatter was observed between the two failure modes. Fiber rupture occurred at $0 < \rho_{frp} E_{frp} < 0.55$ GPa and debonding occurred at $0 < \rho_{frp} E_{frp} < 1.2$ GPa. Authors concluded that debonding dominates over the tensile fracture of the CFRP laminates as they become thicker and stiffer, resulting the necessity of reducing the effective strain. The influence of the concrete strength was also considered when debonding occurs. It was observed that the effective strain in the fibers increased with the increase of the concrete strength. Based on the influence of the concrete strength, another model was derived using the same principle, power regression line (equation 17c). The new reduction factor was obtained by dividing the axial FRP stiffness to the concrete compressive strength. The new model was considered to have better results in terms of r-square, when compared to the results obtained using the other reduction factors.

Bond mechanism model

Proposed for design purposes, the model uses a triangular shape distribution of the shear stresses. Using a simple equilibrium equation for the pure shear stress transfer (not including normal stresses) the total force that can be transferred on two sides and the force at shear failure of the beam are given in equations 18a and b, respectively. Applying the equilibrium condition for the two equations, the strain (stress) reduction factor is determined as shown in equation (18c).

$$(a) \quad T = \frac{1}{2} \tau_{\max} L_e (2 \cdot w_{\text{eff}}); (b) \quad T = 2 t_{frp} w_{\text{eff}} f_{frp,e}; (c) \quad R = \frac{f_{frp,e}}{f_{frp,u}} = \frac{\tau_{\max} L_e}{2 t_{frp} f_{frp,u}} \leq 1 \quad (18a,b,c)$$

where L_e is the effective bond length, set by the authors as being equal to 75 mm. The maximum shear stress was computed as a best-fit polynomial of the concrete compressive strength, resulting:

$$\tau_{\max} = (7.64 f_c^2 \times 10^{-4}) - (2.73 f_c \times 10^{-2}) + 6.38 \quad (19)$$

Aware of the empirical nature of the model, Zhang and Hsu suggested adjustments to the model when more experimental data are available.

2.5 Carolin and Täljsten

The design model of Carolin and Täljsten [12, 13] is based on the superposition principle of the shear contributions of the strengthening and the strut and tie model. A reduction factor to consider the non uniform strain distribution over the cross section was proposed. This reduction factor, η , expresses the average strain in the fibers over the height of the beam in relation to the strain in the most stressed fiber, ε_{\max} .

$$\eta = \frac{\int_{-h/2}^{h/2} \varepsilon_{frp}(y) dy}{\varepsilon_{\max} \cdot h} \quad (20)$$

The reduction factor includes the relative stiffness between concrete in compression, cracked reinforced concrete in tension and lightly reinforced concrete in tension. The proposed design model by Carolin and Täljsten [13] is given as:

$$V_f = \eta \cdot \varepsilon_{cr} \cdot E_{frp} \cdot t_{frp} \cdot r_{frp} \cdot z \cdot \frac{\sin(\theta + \beta)}{\sin \theta} \quad (21)$$

The critical strain, ε_{cr} , is limited by a minimum value of the ultimate allowable fiber capacity, $\varepsilon_{frp,ult}$, the maximum allowable strain without achieving anchorage failure ε_{bond} , and maximum allowable strain to achieve concrete contribution, $\varepsilon_{c,max}$, e.g. concrete contribution due to aggregate interlocking.

$$(a) \quad \varepsilon_{cr} = \min \left\{ \begin{array}{l} \varepsilon_{frp,ult} \\ \varepsilon_{bond} \cdot \sin^2(\theta + \beta) \\ \varepsilon_{c,max} \cdot \sin^2(\theta + \beta) \end{array} \right\}, (b) \quad \varepsilon_{bond} = \frac{1}{E_{frp} t_{frp}} \sqrt{2 E_{frp} t_{frp} G_f} \left\{ \begin{array}{ll} \sin(\omega L_{cr}) & \text{for } L_{cr} \leq \frac{\pi}{2\omega} \\ 1 & \text{for } L_{cr} > \frac{\pi}{2\omega} \end{array} \right. \quad (22a,b)$$

The derivation of the effective strain when debonding occurs (equation (22b)) is presented in [26]. G_f is the concrete fracture energy and ω is defined as:

$$\omega = \sqrt{\frac{\tau_{\max}^2}{2 \cdot E_{frp} \cdot t_{frp} \cdot G_f}} \quad (23)$$

The reduction of $\sin^2(\theta + \beta)$ to the anchorage and concrete contribution comes from the anisotropic behavior of the composite. If the concrete contribution is not included in the shear bearing capacity, the limiting parameter $\varepsilon_{c,max}$ can be ignored. The critical strain times the reduction factor gives the

effective strain, $\varepsilon_{frp,e}$, described earlier. The factor r_{frp} depends on the FRP shear strengthening configuration, being $r_{frp} = \sin\beta$ for whole coverage and $r_{frp} = w/s_{frp}$ for composite strips.

2.6 Monti and Liotta

A complete design method was developed by Monti and Liotta [23] considering all the strengthening schemes and failure modes known at that time. The model was derived by considering three main steps: 1) a generalized FRP-concrete bond constitutive law is defined, 2) boundary limitations are defined, and 3) the stress field in the FRP crossing a shear crack is analytically determined. Also the following assumptions are considered: the cracks are evenly spaced along the beam axis with an inclination of θ , the crack depth is equal to the internal lever arm $z = 0.9d$ for the ultimate limit state, the resisting shear mechanism is based on the truss analogy for wrapping and U-jacketing. For side bonding, the development of a “crack-bridging” resistance mechanism was considered, due to the missing tensile diagonal tie in the truss analogy. The last two assumptions yield that, for wrapping and U-jacketing the truss resisting mechanism can be activated, while for side bonding the role of the FRP is that of “bridging the crack”. The effective bond length (optimal anchorage length), l_e , and the debonding strength, $f_{frp,dd}$ are defined for side bonding.

$$(a) l_e = \sqrt{\frac{E_{frp} t_{frp}}{2f_{ctm}}}; (b) f_{frp,dd} = \frac{0.80}{\gamma_{frp,d}} \sqrt{\frac{2E_{frp} \Gamma_{Fk}}{t_{frp}}} \text{ with } \Gamma_{Fk} = 0.03k_b \sqrt{f_{ck} f_{ctm}} \text{ and} \quad (24a,b)$$

$$k_b = \sqrt{\frac{2 - w / p_{frp}}{1 + w / 400}} \geq 1$$

When sufficient bond length (l_b) cannot be provided due to the strengthening scheme and the apparent shear crack alignment, the bond strength is reduced according to:

$$f_{frp,dd}(l_b) = f_{frp,dd} \frac{l_b}{l_e} \left(2 - \frac{l_b}{l_e} \right) \quad (25)$$

A reduction coefficient, considering the radius of the corner of the beam, is defined for U-jacketing and wrapping as:

$$\varphi_R = 0.2 + 1.6 \frac{r_c}{b} \text{ for } 0 \leq \frac{r_c}{b} \leq 0.5 \quad (26)$$

The ultimate strength of the FRP for all types of strengthening is defined using the following function:

$$f_{frp,ult}(l_b, \delta_e, r_c) = f_{frp,dd}(l_b) + \langle \varphi_R \cdot f_{frp,ult} - f_{frp,dd}(l_b) \rangle \cdot \delta_e \quad (27)$$

If the term in $\langle \cdot \rangle$ of this function becomes negative it should be considered null. Also, a generalized stress-slip constitutive function, $\sigma_{frp}(u, l_b, \delta_e)$, was proposed. The stress-slip law is denoted as a function of the applied slip, u , at the loaded end of the available bond length, l_b , and the end restraint, δ_e . To define the crack width a coordinate system was proposed with the origin placed at the tip of the shear crack and with the abscissa axis along the shear crack. In this way, the crack width, w , can be considered perpendicular to the crack axis. Crack opening is considered to be governed by a linear expression; a slip is imposed to the strip/sheet crossing it.

$$w(x) = \alpha \cdot x \quad (28)$$

Symmetry, with respect to the coordinate system defined above, is considered at both sides of the crack to impose a slip to the FRP crossing this angle. The slip function is given as:

$$u(\alpha, x) = \frac{w(x)}{2} \sin(\theta + \beta) = \frac{1}{2} \alpha x \sin(\theta + \beta) \quad (29)$$

Boundary conditions are imposed as a function of the strengthened scheme adopted i.e. side bonding, U jacketing or wrapping. With the compatibility (crack width) and boundary conditions, the stress

profile in the FRP along the crack $\sigma_{frp,e}(x)$ is determined. In order to determine the FRP contribution to the shear capacity an effective stress along the shear crack length $z/\sin\theta$ is defined as:

$$\sigma_{frp,e}(\alpha) = \frac{1}{z/\sin\theta} \int_0^{z/\sin\theta} \sigma_{frp,cr} [u(\alpha, x), l_b(x)] dx \quad (30)$$

The effective debonding strength, $f_{frp,ed}$, is given by equations (31a), (31b) and (32) for side bonding, for U-jacketing, and for wrapping, respectively.

$$(a) f_{frp,ed} = f_{frp,dd} \frac{z_{rid,eq}}{\min\{0.9d, h_w\}} \left(1 - 0.6 \sqrt{\frac{l_{eq}}{z_{rid,eq}}} \right)^2; (b) f_{frp,ed} = f_{frp,dd} \left(1 - \frac{1}{3} \cdot \frac{l_e \sin \beta}{\min\{0.9d, h_w\}} \right) \quad (31a,b)$$

$$f_{frp,ed} = f_{frp,dd} \left(1 - \frac{1}{6} \frac{l_e \sin \beta}{\min\{0.9d, h_w\}} \right) + \frac{1}{2} (\varphi_R f_{frp,u} - f_{frp,dd}) \left(1 - \frac{l_e \sin \beta}{\min\{0.9d, h_w\}} \right) \quad (32)$$

$$z_{rid,eq} = \min\{0.9d, h_w\} - \left(l_e - \frac{s_f}{f_{frp,dd} / E_{frp}} \right) \sin \beta \quad (33)$$

The FRP contribution to the shear capacity is computed considering two approaches: the Mörsch resisting mechanism for U jacketing and wrapped strengthening schemes (equation (34a)), while for side bonding the “bridging” of the shear crack principle (equation (34b)).

$$(a) V_{frp} = \frac{1}{\gamma_{frp}} 0.9d \cdot f_{frp,ed} 2t_{frp} (\cot \theta + \cot \beta) \frac{w}{\rho_{frp}}; (b) V_{frp} = \frac{1}{\gamma_{frp}} \min\{0.9d, h_w\} f_{frp,ed} 2t_{frp} \frac{\sin \beta}{\sin \theta} \frac{w}{\rho_{frp}} \quad (34a,b)$$

3 DATABASE DESCRIPTION

A full database containing 211 experiments that was collected by Lima and Barros [25] was used to compare the theoretical predictions of the FRP contribution to shear. The database contains values from experiments performed on 91 beams with T cross sections and 120 with rectangular cross sections. With respect to the strengthening configuration the following numbers of elements were identified: 36 fully wrapped; 104 U-wrapped; and 71 side-bonded. For the appraisal of the models performance, beams with a square cross section with the geometrical dimensions smaller than 100x300 mm were removed since these dimensions are unrealistic for shear strengthening. Furthermore, beams with inappropriate material characteristics reported, i.e. of too low concrete compressive and tensile strength, were also removed. In addition, beams containing different anchorage systems were removed since theoretical models do not include the effect of the anchorage systems in their formulations and, consequently, failure predictions are unrealistic.

After removing the values from the database that did not correspond to the above criteria, the theoretical predictions of the models were plotted for the beams reinforced with stirrups (figure 1) and beams without stirrups (figure 2).

4 DISCUSSIONS AND CONCLUSIONS

It is quite clear that existing shear models for FRP strengthening, at least in their present form, do not predict the shear failure very well, see Figures 1 and 2. From the literature it can also be found that many researchers have calibrated their models from unrealistic geometric conditions on their laboratory specimens. No model, as the authors are aware of, considers the interaction between the existing steel stirrups and the FRP wrap, which contributes for level of inaccuracy observed. The Australian guideline proposes a coefficient for this purpose, but noting is reported on how this parameter should be obtained [28].

Consequently, before a more thorough understanding of FRP shear strengthened beams has been obtained a conservative approach is suggested. The question is now how do we go from here? Shear in concrete is complicated, also for non FRP-strengthened beams. Maybe we need to fundamentally rethink how we tackle the FRP shear problem or FRP-strengthening with a conservative approach which may be very expensive.

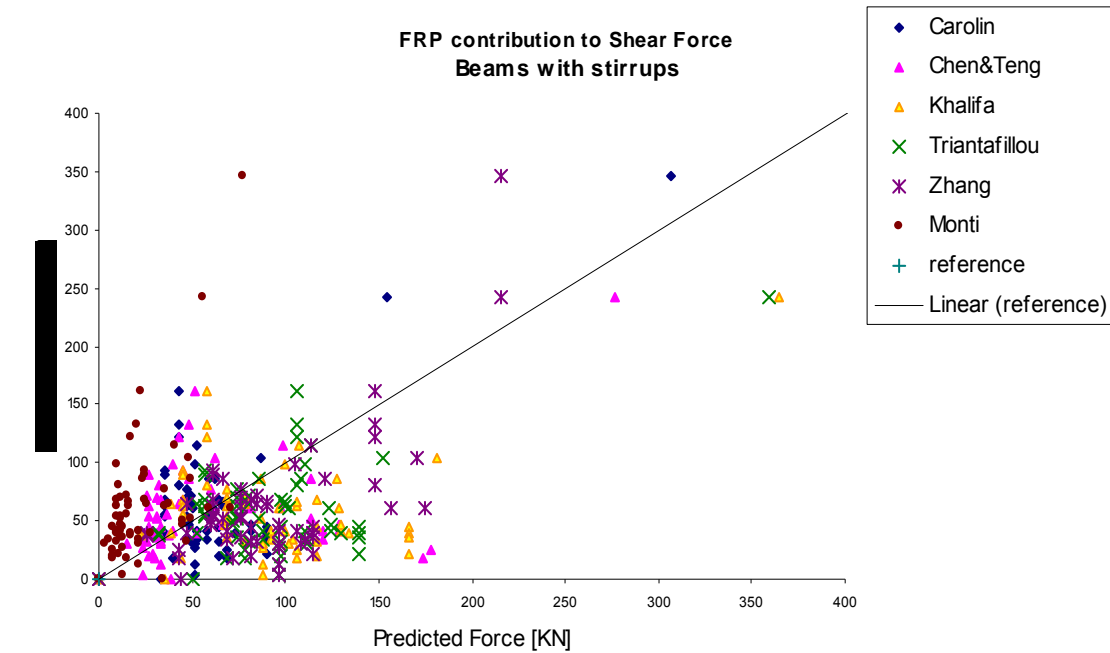


Figure 1: Experimental vs. Theoretical prediction for beams with stirrups.

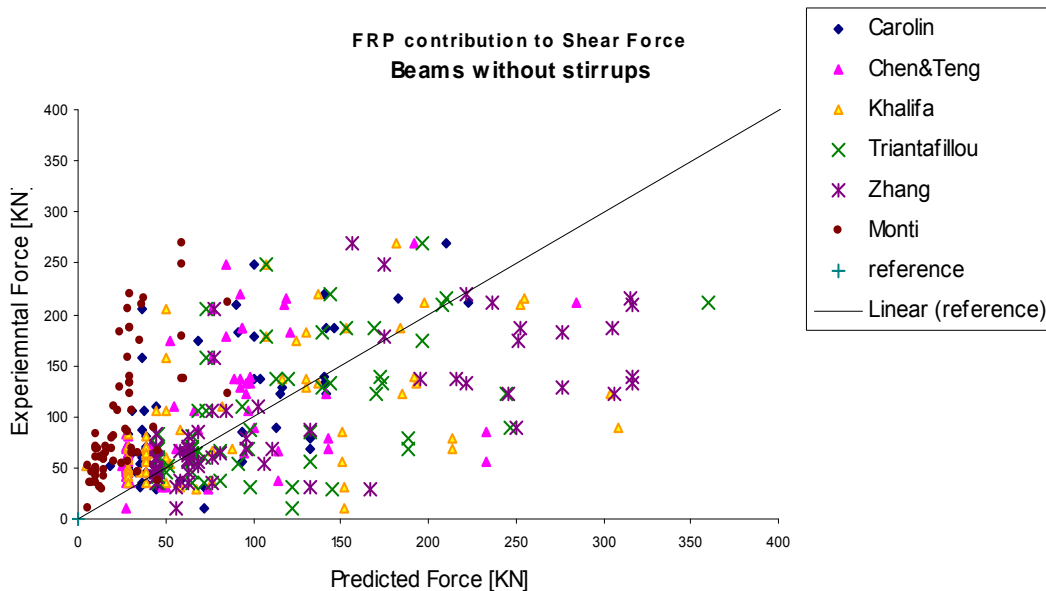


Figure 2: Experimental vs. Theoretical prediction for beams without stirrups.

Furthermore, probably the additional principle cannot be used in its current form when FRP beams are strengthened for shear. Models must be developed that consider interaction between concrete and steel. The existing strain field must be incorporated in the models. Also the change in inclination of the shear cracks when FRP strengthening is used must be further studied.

ACKNOWLEDGMENTS

The authors wish to acknowledge the support provided by the “Empreiteiros Casais”, Degussa, S&P®, Secil (Unibetão, Braga) and Sto Scandinavia AB. The study reported in this paper forms a part of the research program “SmartReinforcement - Carbon fibre laminates for the strengthening and monitoring of reinforced concrete structures” supported by ADI-IDEIA, Project nº 13-05-04-FDR-00031. Part of the study has also been covered within the European network ENCORE (<http://encore.shef.ac.uk/>)

REFERENCES

- [1.] O. Chaallal, M.-J. Nollet, D. Perraton, “Strengthening of reinforced concrete beams with externally bonded fibre-reinforced-plastic plates: design guidelines for shear and flexure”, *Canadian Journal of Civil Engineering*, 25, 692-708 (1998).
- [2.] A. M. Malek, H. Saadatmanesh, “Analytical study of reinforced concrete beams strengthened with web bonded fibre reinforced plastic plates or fabrics”, *ACI Structural Journal*, 95, No. 3, 343-352 (1998a).
- [3.] A. M. Malek, H. Saadatmanesh, “Ultimate shear capacity of reinforced concrete beams strengthened with web-bonded fibre reinforced plastic plates”, *ACI Structural Journal*, 95, No. 4, 391-399 (1998b).
- [4.] T. C. Triantafillou, “Shear Strengthening of reinforced Concrete Beams Using Epoxy-Bonded FRP Composites”, *ACI Structural Journal*, 95, No. 2, 107-115 (1998).
- [5.] T. C. Triantafillou and C. P. Antonopoulos, “Design of concrete flexural members strengthened in shear with FRP” *Journal of Composites for Constructions*, 4, No. 4, 198-205 (2000).
- [6.] A. Khalifa, W. Gold, A. Nanni and M. J. Abdel Aziz, “Contribution of externally bonded FRP to shear capacity of RC flexural members”, *Journal of Composites for Constructions*, 2, No. 4, 195-202 (1998).
- [7.] A. Khalifa, and A. Nanni, “Improving shear capacity of existing RC T-section beams using CFRP composites”, *Cement and Concrete Composites*, 22, No. 3, 165-174 (1999).
- [8.] C. Deniaud and J. J. Roger Cheng, “Shear Behaviour of Reinforced Concrete T-Beams with Externally Bonded Fibre-Reinforced Polymer Sheets”, *ACI Structural Journal*, 98, No. 3, 396-394 (2001).
- [9.] C. Deniaud and J. J. Roger Cheng, “Reinforced Concrete T-Beams Strengthened in Shear with Fibre Reinforced Polymer Sheets”, *Journal of Composites for Construction*, 7, No. 4, 302-310 (2003).
- [10.] C. Deniaud and J. J. Roger Cheng, “Simplified Shear Design Method for Concrete Beams Strengthened with Fibre Reinforced Polymer Sheets”, *Journal of Composites for Construction*, 8, No. 5, 425-433 (2004).
- [11.] C. Pellegrino and C. Modena, “Fiber-Reinforced Polymer Shear Strengthening of Reinforced Concrete Beams: Experimental Study and Analytical Modeling”, *ACI Structural Journal*, 103, No.5, September-October (2006).
- [12.] A. Carolin, *Carbon Fiber Reinforced Polymers for Strengthening of Structural Elements*, Luleå University of Technology, Doctoral thesis 2003:18.
- [13.] A. Carolin, and B. Täljsten, “Experimental Study of Strengthening for Increased Shear Bearing Capacity”, *Journal of Composites for Construction*, 9, No. 6, 488-496 (2005)

- [14.] J. F. Chen and J. G. Teng, "Shear Capacity of Fibre-Reinforced Polymer-Strengthened Reinforced Concrete Beams: Fibre Reinforced Polymer Rupture", *Journal of Structural Engineering*, 129, No. 5, 615-625 (2003a).
- [15.] J. F. Chen and J. G. Teng, "Shear capacity of FRP-strengthened RC beams: FRP debonding", *Construction and Building Materials*, 17, 27-41 (2003b).
- [16.] J. F. Chen and J. G. Teng, "Shear strengthening of RC beams with FRP composites", *Progress in Structural Engineering and Materials*, 6, 173-184 (2004).
- [17.] A. Aprile, A. Benedetti, "Coupled flexural-shear design of R/C beams strengthened with FRP", *Composites: Part B Engineering*, 35, 1-25 (2004).
- [18.] U. Ianniruberto and M. Imbimbo, "Role of Fibre Reinforced Plastic Sheets in Shear Response of Reinforced Concrete Beams: Experimental and Analytical Results", *Journal of Composites for Construction*, 8, No. 5, 415-424 (2004).
- [19.] S. Y. Cao, J. F. Chen, J. G. Teng, Z. Hao and J. Chen, "Debonding in RC Beams Shear Strengthened with Complete FRP Wraps", *Journal of Composites for Construction*, 9, No. 5, 417-428 (2005).
- [20.] Z. Zhang and C.-T. T. Hsu, "Shear Strengthening of Reinforced Concrete Beams Using Carbon-Fibre-Reinforced Polymer Laminates", *Journal of Composites for Construction*, 9, No.2, 158-169 (2005).
- [21.] L. P. Ye, X. Z. Lu and J. F. Chen, "Design Proposals for Debonding Strengths of FRP Strengthened RC Beams in the Chinese Design Code", *Proceedings of International Symposium on Bond Behaviour of FRP in Structures*, Hong Kong, China (2005).
- [22.] C. Pellegrino and C. Modena, "Fibre-Reinforced Polymer Shear Strengthening of Reinforced Concrete Beams: Experimental Study and Analytical Modeling", *ACI Structural Journal*, 103, No. 5, 720-728 (2006).
- [23.] G. Monti and M.A. Liotta, "Tests and design equations for FRP-strengthening in shear", *Construction and Building Materials* (2006), doi:10.1016/j.conbuildmat.2006.06.023.
- [24.] CNR "Instructions for design, execution and control of strengthening interventions through fiber reinforced composites (English version). CNR-DT 200/04, *Consiglio Nazionale delle Ricerche*, Rome, Italy (2005)
- [25.] J.L.T. Lima, J.A.O. Barros, "Design models for shear strengthening of reinforced concrete beams with externally bonded FRP composites: a statistical vs reliability approach", *FRPRCS-8*, University of Patras, Patras, Greece, July 16-18 (2007).
- [26.] T Maeda, Y. Asano, Y. Sato, T. Ueda and Y. Kakuta, "A study on bond mechanism of carbon fiber sheet", *Non metallic (FRP) Reinforcement for Concrete Struct., Proc., 3rd Symp.*, vol. 1, Japan 279-286, (1997)
- [27.] G. Sas, A. Carolin and B. Täljsten, "Model for predicting shear bearing capacity of FRP strengthened beams, *Mechanics of Composite Materials*, submitted for publication, MCM/SI/07003.
- [28.] CIDAR - "Design guideline for RC structures retrofitted with FRP and metal plates: beams and slabs" Draft 3 - submitted to Standards Australia, The University of Adelaide, (2006).

NOTATION LIST

γ_{frp}	partial safety factor for the tensile strength of FRP
b_w	minimum width of CS over the effective depth
d	effective depth of the CS
β	fibre angle direction with respect to the longitudinal axis of the beam
$\varepsilon_{frp,e}$	effective FRP strain at failure
t_{frp}	thickness of the FRP
E_{frp}	the elastic modulus of FRP
f_c	Concrete compressive strength
w_{frp}	width of the FRP
θ	crack angle direction with respect to the longitudinal axis of the beam
d_{frp}	effective depth of FRP over the height of the beam
$f_{frp,e}$	effective tensile stress in FRP
$h_{frp,e}$	the effective height of the FRP bonded on the web
h	height of the beam
d_t	is the distance from the compression face to the top edge of the FRP
d_c	the distance from the compression face to the lower edge of the FRP
$f_{frp,u}$	Ultimate tensile strength of FRP
γ_b	the partial safety factor for bond strength equals 1.25
$\varepsilon_{frp,u}$	ultimate tensile strain of FRP
ε_{cr}	is the critical strain
τ_{max}	is the maximum shear stress of concrete
$\gamma_{frp,d}$	is a partial safety factor depending on application quality
s_{frp}	is the distance between the FRP strips/sheets
w	is the width measured orthogonally to β
l_e	is the effective bond length
$f_{frp,dd}$	is the debonding strength
α	is the crack opening angle
$f_{frp,ed}$	is the effective debonding strength
h_w	Is the height of the web of a T beam
η	equals to 0.6 is the strain reduction factor
z	is the length of the vertical tension tie in the truss, normally expressed as $0.9d$.
ε_{cr}	is the critical strain.
f_{ck}	is the concrete characteristic cylinder strength
R_{ck}	is the concrete characteristic cube strength
f_{ctm}	is the mean tensile strength of concrete computed as $0.27 (R_{ck})^{2/3}$
Γ_{Fk}	is the specific fracture energy of the FRP to concrete bond interface
ρ_{frp}	is the spacing measured orthogonally to β
δ_e	is the radius coefficient. Equals 0 for free end and 1 for wrapped around the corner
$z_{rid,eq}$	is equal to the vertically projected length of the FRP minus the entire length